

Cationic palladium(II)–acetylacetone complexes bearing pyridinyl imine ligands as catalysts for the hydroamination of phenylacetylene and polymerization of norbornene

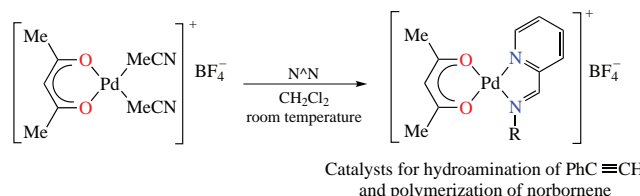
Dmitrii S. Suslov,^a Anastasia V. Suchkova,^a Mikhail V. Bykov,^a Zorikto D. Abramov,^a Marina V. Pakhomova,^a Timur S. Orlov,^a Igor A. Ushakov,^b Tatyana N. Borodina^b and Vladimir I. Smirnov^b

^a Research Institute of Oil and Coal Chemical Synthesis, Irkutsk State University, 664003 Irkutsk, Russian Federation. E-mail: suslov@chem.isu.ru, suslov.dmitry@gmail.com

^b A. E. Favorsky Irkutsk Institute of Chemistry, Siberian Branch of the Russian Academy of Sciences, 664033 Irkutsk, Russian Federation

DOI: 10.1016/j.mencom.2023.02.011

Acetylacetone palladium(II) complexes bearing pyridinyl imine ligands $[\text{Pd}(\text{acac})(\text{L})]\text{BF}_4$ were synthesized *via* nitrile displacement in $[\text{Pd}(\text{acac})(\text{MeCN})_2]\text{BF}_4$ by the bidentate ligands **L** of type $2\text{-C}_5\text{H}_4\text{N}-\text{CH}=\text{N}-(\text{CH}_2)_n\text{OMe}$ or $2\text{-C}_5\text{H}_4\text{N}-\text{CH}=\text{N}-\text{Ar}$. The structures of complexes were analyzed by X-ray diffractometry, NMR, and DFT. The complexes catalyze hydroamination of phenylacetylene with aniline to give the Markovnikov imine product as well as polymerization of norbornene.



Keywords: palladium, acetylacetone, imines, pyridines, norbornene, phenylacetylene, hydroamination, polymerization.

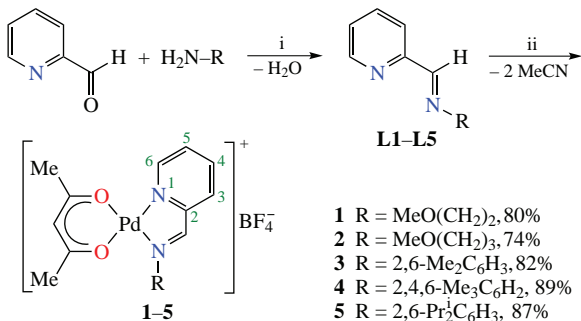
This paper is dedicated to Academician Irina Petrovna Beletskaya on the occasion of her anniversary – the outstanding Russian organic chemist, whose contributions have vastly enriched the application and theory of transition metal catalysis in organic synthesis.

Among metal-based catalysts, complexes with Schiff base ligands belong to a very important group because of their multifunctionality and versatility. Particular attention has been directed toward nitrogen-donor late transition metal complexes as a result of Brookhart's report on Pd^{II} and Ni^{II} diimine catalyst systems^{1,2} for polymerization of olefins. Later, the discovery, made by Brookhart and Gibson, that iron and cobalt complexes bearing bis(imino) pyridine ligands are also effective catalyst for converting olefins to high molecular weight polymers^{3–5} led to the development of a number of nitrogen-donor ligands belonging to the family of iminopyridines.

Having a long-standing interest in cationic acetylacetone palladium complexes,^{6–12} we have prepared herein imino pyridine-chelated complexes of the form $[\text{Pd}(\text{acac})(\text{N}^{\text{+}}\text{N}')]\text{BF}_4$ **1–5** (Scheme 1). Their structural features and aspects of their

application as precatalyst for the addition polymerization of norbornene and hydroamination of phenylacetylene with aniline were also studied. Reactions of equimolar amounts of ligands **L1–L5** with bis(acetonitrile)(acetylacetone)palladium(II) tetrafluoroborate in dichloromethane led to complexes **1–5** as yellow solids in high yields. New compounds **1**, **2**, **4**, and **5** were fully characterized by NMR spectroscopy, ESI-MS, and elemental analysis (see Online Supplementary Materials). Known¹³ compound **3** was prepared herein in a more facile synthetic route in less steps without usage of toxic thalium salts.

Generally, the δ values in ^1H and ^{13}C NMR spectra of complexes **1–5** are consistent with NMR data for the ligands or for the corresponding transition metal complexes.^{13–20} On moving from ligands **L1–L5** to complexes **1–5**, the most affected protons are H^4 and H^5 from pyridine ring whose signals would shift downfield by 0.47–0.64 ppm upon coordination to Pd (see Online Supplementary Materials, Table S1). In contrast to dichloride analogues^{16,21} where the 6-positioned proton signals are shifted upfield upon complexation, the chemical shifts for H^6 in ligands **L1–L5** vs. cationic acetylacetone complexes **1–5** are essentially close. Interesting structural feature reported for the imino pyridine palladium complexes is hindered rotation of the aryl substituent of the imino nitrogen atom.^{16,18,21} Consequently, the doublet from the isopropyl group of the free ligand at $\delta = 1.17$ ppm¹⁶ has been split into two doublets in the case of complex **5**, which may be explained by the blocking effect of the acetylacetone ligand. Despite the fact that DFT calculations data (on the BP86/def2-TZVP_{Pd}/def2-SVP_{C,H,N,O} level, see Figure S56) for cations of **1** or **2** suggest the presence of two



Scheme 1 Reagents and conditions: i, MgSO_4 , Et_2O , room temperature, 4 h; ii, $[\text{Pd}(\text{acac})(\text{MeCN})_2]\text{BF}_4$, CH_2Cl_2 , room temperature, 3 h.

isomers (one with the OMe group located close to the axial position of the coordination polyhedron), only one isomer has been detected by NMR.

NOE relationships found in the $\{^1\text{H}-^1\text{H}\}$ NOESY spectra (see example sketched on Figure S45), as well as two-dimensional C–H hetero-correlations have allowed full assignment of ^1H and $^{13}\text{C}\{^1\text{H}\}$ -NMR signals for complexes **1–5** (see Figures S3–S44). The lower symmetry of the pyridinyl imine ligands causes the nonequivalence of the two methyl groups in acetylacetone fragment. The distinctive proton signal resonances at, for example, 2.22 (**1**), 2.20 (**5**) and 2.26 (**1**), 1.72 (**5**) ppm (the last shielded by aromatic ring current) from Me-group of acac ligand were observed in the ^1H NMR spectra (see Online Supplementary Materials, Table S1). In addition, the $^{13}\text{C}\{^1\text{H}\}$ NMR spectra revealed the appearance of diagnostic carbon peaks of acac for carbonyl and methyl groups, which were split by the adjacent pyridinyl moiety of the ligands. As an example, in the $^{13}\text{C}\{^1\text{H}\}$ NMR spectrum of **4** carbonyl groups appear at 188.38 and 187.65 ppm, and methyl groups resonate at 25.69, 26.23 ppm in the *trans*- and *cis*-position with regard to the N atom of pyridine ring, respectively (Figures S29, S32, S45).

The ^{15}N NMR spectra were recorded for complexes **1–5** and ligands **L1**, **L2** by $\{^1\text{H}, ^{15}\text{N}\}$ -HMBC experiments on the natural abundance of the ^{15}N isotope (see Online Supplementary Materials, ^{15}N NMR data were not previously reported^{14,15,19} for the ligands **L1** and **L2**). The chemical shifts in the complexes were assigned mainly through the cross peaks with the resonances of the ligand protons. ^{15}N NMR experiments (Table S2) clearly prove that the nitrogen donor atoms of **1–5** are coordinating. In all cases coordination of the nitrogen atoms resulted in an upfield shift $\Delta(\delta_{\text{complex}} - \delta_{\text{ligand}})$ of the ^{15}N NMR signals in the range of –83 to –100 ppm. It is known that the coordination-induced shift of a nitrogen atom in palladium complexes is mainly dependent on the σ -donor capacities of a ligand that is in a *trans* position.^{22,23} For example, values of *ca.* –90 ppm have been observed for weakly σ -donating ligands (*e.g.*, a chloride atom).²⁴

Single crystals of complexes **3** and **5** suitable for X-ray crystallography (Figure 1)[†] were obtained by diffusion of Et_2O vapour into solutions of the complexes in 1,2-dichloroethane. Despite attempts of crystallization, the quality of crystals of **4** was not sufficient to avoid the disorder of the $[\text{BF}_4]^-$ anions (Figure S56, Tables S6 and S7). Complexes **3** and **5** contain a four-coordinate palladium(II) centre with a non-coordinating $[\text{BF}_4]^-$ anion. The asymmetric unit of **3** contains two independent molecular entities, whereas only one molecule is found in the asymmetric unit of complex **5**. The overall geometry around

[†] Crystal data for **3**. $\text{C}_{19}\text{H}_{21}\text{N}_2\text{O}_2\text{Pd}, \text{BF}_4$, 502.59 g mol^{–1}, orthorhombic, space group $C222_1$, $a = 11.476(10)$, $b = 29.30(3)$ and $c = 25.25(2)$ Å, $V = 8490(13)$ Å³, $Z = 16$, $T = 293(2)$ K, $\mu(\text{MoK}\alpha) = 0.925$ mm^{–1}, $d_{\text{calc}} = 1.573$ g cm^{–3}, 24321 reflections measured, 12329 unique ($R_{\text{int}} = 0.0574$). The final $R_1 = 0.0520$, $wR_2 = 0.1060$ [$I > 2\sigma(I)$] and $R_1 = 0.1250$, $wR_2 = 0.1383$ (all data), $\text{GooF} = 0.991$. Largest diff. peak/hole 0.56/–0.53 e Å^{–3}.

Crystal data for **5**. $\text{C}_{23}\text{H}_{29}\text{N}_2\text{O}_2\text{Pd}, \text{BF}_4$, 558.69 g mol^{–1}, monoclinic, space group $P21/n$, $a = 8.679(4)$, $b = 16.948(9)$ and $c = 17.691(9)$ Å, $\beta = 103.378(15)$ °, $V = 2532(2)$ Å³, $Z = 4$, $T = 293(2)$ K, $\mu(\text{MoK}\alpha) = 0.784$ mm^{–1}, $d_{\text{calc}} = 1.466$ g cm^{–3}, 76229 reflections measured, 7445 unique ($R_{\text{int}} = 0.0534$). The final $R_1 = 0.0379$, $wR_2 = 0.1013$ [$I > 2\sigma(I)$] and $R_1 = 0.0547$, $wR_2 = 0.1117$ (all data), $\text{GooF} = 1.038$. Largest diff. peak/hole 0.70/–0.51 e Å^{–3}.

Data were collected on a Bruker D8 Venture Photon 100 CMOS diffractometer with $\text{MoK}\alpha$ radiation ($\lambda = 0.71073$ Å) using the ϕ and ω scans technique.

CCDC 2162440 and 2162442 contain the supplementary crystallographic data for this paper. These data can be obtained free of charge from The Cambridge Crystallographic Data Centre via <http://www.ccdc.cam.ac.uk>.

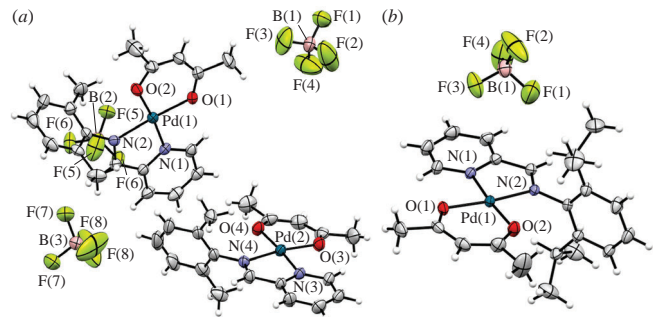
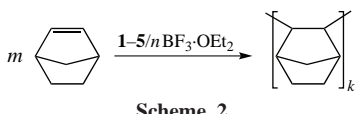


Figure 1 ORTEP plot of (a) compound **3** and (b) compound **5** with atoms represented by thermal vibration ellipsoids of 25% probability. Selected bond distances (Å) and angles (°) for the cations in **3**: $\text{Pd}(1)-\text{N}(1) = 2.000(5)$, $\text{Pd}(1)-\text{N}(2) = 2.007(5)$, $\text{Pd}(1)-\text{O}(1) = 1.976(4)$, $\text{Pd}(1)-\text{O}(2) = 1.959(5)$, $\text{Pd}(2)-\text{N}(3) = 1.983(5)$, $\text{Pd}(2)-\text{N}(4) = 2.007(5)$, $\text{Pd}(2)-\text{O}(3) = 1.964(5)$, $\text{Pd}(2)-\text{O}(4) = 1.966(4)$, $\angle\text{N}(1)-\text{Pd}(1)-\text{N}(2) = 81.0(2)$, $\angle\text{O}(2)-\text{Pd}(1)-\text{O}(1) = 94.2(2)$, $\angle\text{N}(3)-\text{Pd}(2)-\text{N}(4) = 80.7(2)$, $\angle\text{O}(3)-\text{Pd}(2)-\text{O}(4) = 93.5(2)$; in **5**: $\text{Pd}(1)-\text{N}(1) = 1.995(2)$, $\text{Pd}(1)-\text{N}(2) = 1.993(2)$, $\text{Pd}(1)-\text{O}(1) = 1.972(2)$, $\text{Pd}(1)-\text{O}(2) = 1.956(2)$, $\text{N}(2)-\text{Pd}(1)-\text{N}(1) = 80.91(8)$, $\angle\text{O}(2)-\text{Pd}(1)-\text{O}(1) = 94.12(8)$.

Pd in the complexes is approximately square planar, with the distortion arising from the relatively small $\text{N}_i-\text{Pd}-\text{N}_{i+1}$ bite angle (*ca.* 81°). The angles between the mean plane defined by the imino aromatic ring with respect to the coordination plane of the palladium atom (defined by the atoms N_i , N_{i+1} , and Pd) fall in the range of 71 to 83°. Because of this orientation, the free space in the coordination sphere around palladium is partly controlled by the imino aryl substituents.¹⁷ Another common structural feature between the palladium complexes is length of imino double bond. Relative to other bonds in the imino bridge, the C=N bond in compounds of this study is the shortest ([1.264(8), 1.278(7)] and 1.278(3) Å, for **3** and **5**, respectively). To gain more insight into the structure of the cationic species, we performed DFT (BP86) calculations for the cations of **3** and **5** in gas phase, hence, free from the influence of crystal packing or intermolecular interactions. Within the limits of the basis set employed, the optimized geometries were good representation of the structures obtained from the crystallographic studies. DFT calculations showed maximum Mayer bond orders for the C=N bond indicating low imino double bond delocalization (*e.g.*, 1.5991 and 1.5746 for cations of **3** and **5**, respectively; in ligands (*cis/trans*) **L3** and **L5**, the Mayer bond orders of *ca.* 1.80–1.84 were calculated).

The average Pd–N bond lengths in complexes **3** and **5** of 1.999 and 1.994 Å are close to those of previously reported for cationic palladium(II) acetylacetone complex¹³ (2.009 Å), but slightly shorter when compared to chloride analogues with $(\text{Pd}-\text{N})_{\text{av}}$ bond length of 2.024 Å.^{16,21} The palladium atom is situated in the coordination plane $\text{N}_i-\text{N}_{i+1}-\text{O}_i-\text{O}_{i+1}$ (0.021 and 0.002 Å above the calculated plane in **3** and **5**). The $\text{O}_i-\text{Pd}_j-\text{O}_{i+1}$ angle is in the range of 93.5 to 94.2°, which is the normal bite angle for acetylacetone palladium complexes.^{10,13} In complexes **3** and **5** the Pd–O bond distance *trans* to nitrogen atom of imine group is slightly longer than the other one [$l(\text{Pd}(1)-\text{O}(1)) = 1.972(2)$ vs. $l(\text{Pd}(1)-\text{O}(2)) = 1.956(2)$ Å]. Analysis of the bond lengths and angles of $[\text{BF}_4]^-$ ion (Tables S4 and S5) showed distortion of the idealized tetrahedral geometry. In addition, short contacts between the fluorine atoms of $[\text{BF}_4]^-$ and the hydrogens of the imine moiety ($\text{F}\cdots\text{H}-\text{C}=\text{N}$, 2.3 Å) are observed in the crystallographic packing of **3** and **5**, thus presumably forming weak C–H···F hydrogen bonds.

Polynorbornene (PNB) has received considerable attention due to its dielectric and mechanical properties for technical application as an interlevel dielectric in microelectronics



Scheme 2

Table 1 Polymerization of norbornene (NB) catalyzed by complexes 1–5.^a

Entry	Complex	T/°C	t/min	Solvent	Yield of PNB (%)	TON ^b	A ^c
1	1	25	240	CH ₂ Cl ₂	66.1	3300	77.8
2	2	25	240	CH ₂ Cl ₂	81.5	4070	95.9
3	3	25	240	CH ₂ Cl ₂	6.8	340	8.0
4	4	25	240	CH ₂ Cl ₂	23.6	1180	27.9
5	5	25	240	CH ₂ Cl ₂	4.8	240	5.6
6	2	10	10	Cl(CH ₂) ₂ Cl	2.8	140	79.4
7	2	25	10	Cl(CH ₂) ₂ Cl	7.6	380	214.8
8	2	50	10	Cl(CH ₂) ₂ Cl	33.6	1680	946.4
9	2	75	10	Cl(CH ₂) ₂ Cl	65.8	3290	1853.7
10	2	100	10	Cl(CH ₂) ₂ Cl	80.6	4030	2271.5

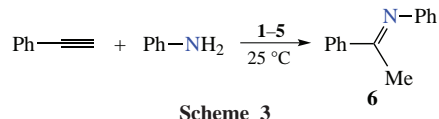
^a Conditions: BF₃·OEt₂ (50 equiv.), *n*_{NB} = 23 mmol, *n*_{complex} = 4.6 μmol, [NB]₀/[Pd]₀ = 5000, *V*₀ = 9 mL. ^b TON in (mol NB) (mol Pd)⁻¹. ^c Average activity of the catalyst in (g_{NB}) × 10⁻³ (mol_{Pd} h)⁻¹.

applications.^{25–28} A variety of palladium complexes have been found active for the polymerization of norbornene,^{25,28} but the applications of imino pyridine-chelated palladium complexes in this reaction are rare.^{21,25,26,28} Cationic palladium complexes **1–5** were screened for their ability to polymerize norbornene (NB, Scheme 2). The complexes were activated with BF₃·OEt₂. Preliminary experiments showed that neither **1–5** nor BF₃·OEt₂ could catalyze the polymerization. It is known that β-diketonate Pd-complexes activated with BF₃·OEt₂ have shown promising results for polymerization of NB and its derivates.^{12,25,26,28} The polymerization activities for **1–5** cover the range from 5.6×10^3 g_{PNB} (mol Pd)⁻¹ h⁻¹ (Table 1, entry 5) to 2.2×10^6 (mol Pd)⁻¹ h⁻¹ (entry 10) which can be classified as low to high.²⁵ Table 1 shows that norbornene polymerization runs with complexes **3–5** are significantly slower than the runs with **1** and **2**. This can be attributed to the steric factors when the bulky aryl substituent in **3–5** being almost perpendicular with respect to the mean coordination plane would hinder the norbornene coordination and thus would slow the NB-insertion rate. Previously, it has been shown that NB-coordination step is rate-determining for NB polymerization with cationic palladium complexes bearing amino pyridine ligands.²⁹ The most active complex **2** was chosen as the precatalyst for the study of the polymerization in detail (Figure S58), when the monomer conversion reached 71% at 240 min. The pseudo-first-order plot was linear, and TOF₀ = 12.4 min⁻¹ was calculated. As results a linear relation between activity and the initial molar ratio of NB to **2** of up to [NB]₀/[Pd]₀ of 7500 was found (Figure S59). Variation of the ratio between BF₃·OEt₂ and **2** showed considerable effect on the catalytic activities (Figure S61). When the [NB]/[Pd] ratio was increased, the catalytic ability of **2** first increased rapidly and then increases smoothly. It was found that the activity of **2** increased with the temperature raising from 25 to 100 °C (see Table 1, entries 6–10). The highest activity was found at 100 °C indicating that the active species were stable at high temperature. Molecular weights of the obtained polymers could not be determined by gel permeation chromatography due to insolubility of the products in organic solvents including 1,2,4-trichlorobenzene. Insolubility of addition PNBs is frequently observed. The origin of this insolubility is not clear, one possibility may be chain cross-linking due to partial cationic polymerization or tacticity.³⁰ IR (KBr disk) analysis of PNB (Figure S63) showed no absorbance in the 1600–1670 cm⁻¹

range, indicating that polymerization occurred *via* a vinyl addition pathway.³¹

One of the most attractive strategies for the preparation of amines is the catalytic hydroamination of unsaturated compounds. Numerous catalysts have been developed to promote the intermolecular catalytic hydroamination of terminal acetylenes,³² whereas palladium catalysts among them are rare enough.^{33–39} In most cases these catalysts operate at elevated temperatures and require acidic additives. Although palladium complexes with bidentate imino pyridine ligands have been applied for alkene oligo- and polymerization,^{15,20,21,40} alkoxy-carbonylation,^{17,41} and synthesis of polyketones,¹⁹ we were unable to find reports of their application as catalyst for hydroamination alkynes.

To further investigate the catalytic activity of **1–5**, the intermolecular hydroamination of phenylacetylene (PA) with aniline (AN) was examined (Scheme 3, Table 2). The reactions were performed under solvent-free conditions with a slight excess of aniline with respect to PA, *i.e.* the same reaction conditions previously applied with one of the most productive (TON = 550) palladium catalyst bearing Anthraphos ligands.³⁸ In our experiments all complexes generated active catalysts showing a remarkable effect of the pyridinyl imine ligand on the productivity and chemoselectivity. In all cases, the Markovnikov product, *N*-(1-phenylethylidene)benzenamine **6**, was obtained exclusively. Complexes **1** and **2** were the least productive, while the highest value of TON = 295 was obtained with **5** (see Table 2, entry 5). Also, catalysts **3** and **4** which were tested under the same reaction conditions, afforded a slightly lower productivity. Next, the precatalysts were studied under different reaction conditions. In the case of **4**, at 70 °C higher productivity was obtained (TON = 225, chemoselectivity of 45%; entry 9) compared to the results at higher temperatures (Table S8). When PA was added in a threefold excess with respect to aniline, the product yields were more synthetically useful (see Table 2, entry 12). But in the case of complexes **1** and **2**, yields and selectivity were low. Most hydroamination catalysts (including state-of-the-art-type) also promote oligomerization of alkynes, so the yields are mostly calculated based on the N–H nucleophile



Scheme 3

Table 2 Hydroamination of phenylacetylene with aniline catalyzed by complexes **1–5**.

Entry ^a	Pd	T/°C	t/h	Conversion of PA (%)	Yield of 6 ^b (%)	Selectivity (%) ^c	TON ^d
1	1	25	168	50	16	32	85
2	2	25	168	47	13	28	70
3	3	25	168	92	54	59	285
4	4	25	168	92	53	58	280
5	5	25	168	89	56	63	295
6	1	70	15	49	12	24	65
7	2	70	15	55	14	25	75
8	3	70	15	97	42	43	225
9	4	70	15	94	42	45	225
10	5	70	15	96	43	45	230
11	5	70	3	74	29	39	155
12 ^e	5	70	3	43	79	46	258

^a Conditions: 0.086 mol% of Pd, [PA]₀/[AN]₀/[Pd]₀ = 530/630/1, *n*_{Pd} = 8.6 μmol, *V*₀ = 1.0 mL. ^b GC yield measured with benzene as internal standard. ^c Chemoselectivity = *n*₆(*n*_{PA})⁻¹. ^d In units of (mol of **6**)(mol of Pd)⁻¹. ^e [PA]₀/[AN]₀/[Pd]₀ = 1300/325/1, 0.062 mol% of Pd.

as the alkyne is added in excess.³² We also observed oligomerization of the alkyne as the side reaction. The oligomers precipitated in acidified MeOH as yellow or brown solids. Therefore, the growth in chemoselectivity from **1** to **5** is reasonably ascribed to the increasing steric bulk in the coordination sphere of the metal and preventing PA coordination, which is in agreement with the NB polymerization (see above). In addition, complexes **1** and **2** initiate phenylacetylene oligomerization in neat monomer (Table S9). Intriguingly, complexes **3–5** gave oligomers only in the presence of aniline.

To explain the effect of the ligand nature on the productivity and chemoselectivity, the propagation and termination steps of the catalytic cycle will be considered. Two potential mechanisms known³² for palladium catalysts are outlined in Figure S68 (see Online Supplementary Materials). Path A involves activation of the C–C multiple bond by π -coordination of a Lewis-acidic metal complex, followed by nucleophilic addition of the N-nucleophile. Subsequent protolytic cleavage of the metal–carbon bond provides the enamine product, which dissociates from the coordination sphere of the metal. The resulting enamine isomerizes to the corresponding imine. On the other hand, an amine activation pathway cannot be excluded. Path B involves initial formation of a metal–nitrogen bond, followed by insertion of the alkyne into the M–N bond. Despite the mechanism in Path B is rather tentative, it seems to be preferable, since explains the formation of phenylacetylene oligomers only in the presence of aniline.

In conclusion, we have synthesized four new cationic acetylacetone palladium complexes $[\text{Pd}(\text{acac})(\text{L})][\text{BF}_4^-]$ (L is bidentate pyridinyl imine ligand). The catalytic potential of the complexes was demonstrated in the addition polymerization of norbornene and intermolecular hydroamination of phenylacetylene with aniline. Though the present research was limited to the study of the reactions mentioned above, we believe these novel precatalysts may have a broad potential for a variety of other catalytic applications.

This work was supported by the Government Assignment for Scientific Research from the Ministry of Science and Higher Education of the Russian Federation (FZZE-2023-0006). Mikhail V. Bykov acknowledges Ministry of Science and Higher Education of the Russian Federation for scholarship (no. 54 of 26.01.2021). We thank Dr. A. V. Kuzmin for ESI-MS measurements. We thank Mr. D. K. Zhuravlev and Mr. V. I. Butorin for experimental support. The studies were performed utilizing equipment from the Baikal Analytical Center of Collective Use SB RAS (<http://ckp-rf.ru/ckp/3050/>), the Center for Collective Use of Analytical Equipment of Irkutsk State University (<http://ckp-rf.ru/ckp/3264/>), and the Shared Research Facilities for Physical and Chemical Ultramicroanalysis LIN SB RAS.

Online Supplementary Materials

Supplementary data associated with this article can be found in the online version at doi: 10.1016/j.mencom.2023.02.011.

References

1. L. K. Johnson, C. M. Killian and M. S. Brookhart, *J. Am. Chem. Soc.*, 1995, **117**, 6414.
2. S. D. Ittel, L. K. Johnson and M. S. Brookhart, *Chem. Rev.*, 2000, **100**, 1169.
3. V. C. Gibson and S. K. Spitzmesser, *Chem. Rev.*, 2003, **103**, 283.
4. G. J. P. Britovsek, S. Mastroianni, G. A. Solan, S. P. D. Baugh, C. Redshaw, V. C. Gibson, A. J. P. White, D. J. Williams and M. R. J. Elsegood, *Chem. – Eur. J.*, 2000, **6**, 2221.
5. V. C. Gibson, C. Redshaw and G. A. Solan, *Chem. Rev.*, 2007, **107**, 1745.
6. V. S. Tkach, D. S. Suslov, G. Myagmarsuren, G. V. Ratovskii, A. V. Rohin, F. Tuczek and F. K. Shmidt, *J. Organomet. Chem.*, 2008, **693**, 2069.
7. D. S. Suslov, M. V. Bykov, P. A. Abramov, M. V. Pakhomova, I. A. Ushakov, V. K. Voronov and V. S. Tkach, *Inorg. Chem. Commun.*, 2016, **66**, 1.
8. D. S. Suslov, M. V. Bykov, M. V. Belova, P. A. Abramov and V. S. Tkach, *J. Organomet. Chem.*, 2014, **752**, 37.
9. D. S. Suslov, M. V. Bykov, Z. D. Abramov, I. A. Ushakov, T. N. Borodina, V. I. Smirnov, G. V. Ratovskii and V. S. Tkach, *J. Organomet. Chem.*, 2020, **923**, 121413.
10. D. S. Suslov, Z. D. Abramov, I. A. Babenko, V. A. Bezborodov, T. N. Borodina, M. V. Bykov, M. V. Pakhomova, V. I. Smirnov, A. V. Suchkova, G. V. Ratovskii, I. A. Ushakov and A. I. Vilms, *Appl. Organomet. Chem.*, 2021, **35**, e6381.
11. D. S. Suslov, M. V. Bykov, M. V. Pakhomova, P. A. Abramov, I. A. Ushakov and V. S. Tkach, *Catal. Commun.*, 2017, **94**, 69.
12. D. S. Suslov, M. V. Bykov, A. V. Kuzmin, P. A. Abramov, O. V. Kravchenko, M. V. Pakhomova, A. V. Rokhin, I. A. Ushakov and V. S. Tkach, *Catal. Commun.*, 2018, **106**, 30.
13. T. Birkle, A. Carbayo, J. V. Cuevas, G. García-Herbosa and A. Muñoz, *Eur. J. Inorg. Chem.*, 2012, **2**, 2259.
14. S. A. Turner, Z. D. Remillard, D. T. Gijima, E. Gao, R. D. Pike and C. Goh, *Inorg. Chem.*, 2012, **51**, 10762.
15. G. S. Nyamato, S. O. Ojwach and M. P. Akerman, *Organometallics*, 2015, **34**, 5647.
16. T. V. Laine, M. Klinga and M. Leskelä, *Eur. J. Inorg. Chem.*, 1999, 959.
17. C. Bianchini, H. M. Lee, G. Mantovani, A. Meli and W. Oberhauser, *New J. Chem.*, 2002, **26**, 387.
18. J. Cámpora, M. del Mar Conejo, K. Mereiter, P. Palma, C. Pérez, M. L. Reyes and C. Ruiz, *J. Organomet. Chem.*, 2003, **683**, 220.
19. V. Rosar, D. Dedeic, T. Nobile, F. Fini, G. Balducci, E. Alessio, C. Carfagna and B. Milani, *Dalton Trans.*, 2016, **45**, 14609.
20. S. Park, J. Lee, J. H. Jeong, H. Lee and S. Nayab, *Polyhedron*, 2018, **151**, 82.
21. T. V. Laine, U. Piironen, K. Lappalainen, M. Klinga, E. Aitola and M. Leskelä, *J. Organomet. Chem.*, 2000, **606**, 112.
22. R. E. Rükle, J. M. Ernsting, A. L. Spek, C. J. Elsevier, P. W. N. M. van Leeuwen and K. Vrieze, *Inorg. Chem.*, 1993, **32**, 5769.
23. P. S. Pregosin, R. Rüedi and C. Anklin, *Magn. Reson. Chem.*, 1986, **24**, 255.
24. L. Pazderski, in *Annual Reports on NMR Spectroscopy*, ed. G. Webb, Elsevier, Amsterdam, 2013, vol. 80, pp. 33–179.
25. F. Blank and C. Janiak, *Coord. Chem. Rev.*, 2009, **293**, 827.
26. M. V. Bermeshev and P. P. Chapala, *Prog. Polym. Sci.*, 2018, **84**, 1.
27. V. R. Flid, M. L. Gringolts, R. S. Shamsiev and E. S. Finkelshtein, *Russ. Chem. Rev.*, 2018, **87**, 1169.
28. D. S. Suslov, M. V. Bykov and O. V. Kravchenko, *Polym. Sci., Ser. C*, 2019, **61**, 145 (*Vysokomol. Soedin., Ser. C*, 2019, **61**, 122).
29. K.-H. Yu, S.-L. Huang, Y.-H. Liu, Y. Wang, S.-T. Liu, Y.-C. Cheng, Y.-F. Lin and J.-T. Chen, *Molecules*, 2017, **22**, 1095.
30. F. Blank, J. K. Vieth, J. Ruiz, V. Rodríguez and C. Janiak, *J. Organomet. Chem.*, 2011, **696**, 473.
31. X. Mi, Z. Ma, N. Cui, L. Wang, Y. Ke and Y. Hu, *J. Appl. Polym. Sci.*, 2003, **88**, 3273.
32. L. Huang, M. Arndt, K. Gooßen, H. Heydt and L. J. Gooßen, *Chem. Rev.*, 2015, **115**, 2596.
33. D. Franco, A. Marchenko, G. Koidan, A. N. Hurieva, A. Kostyuk and A. Biffis, *ACS Omega*, 2018, **3**, 17888.
34. A. Casnati, A. Voronov, D. G. Ferrari, R. Mancuso, B. Gabriele, E. Motti and N. Della Ca, *Catalysts*, 2020, **10**, 176.
35. Q. Chen, L. Lv, M. Yu, Y. Shi, Y. Li, G. Pang and C. Cao, *RSC Adv.*, 2013, **3**, 18359.
36. J. C. Bernhammer, N. X. Chong, R. Jothibusu, B. Zhou and H. V. Huynh, *Organometallics*, 2014, **33**, 3607.
37. M. Virant, M. Mihelač, M. Gazvoda, A. E. Cotman, A. Frantar, B. Pinter and J. Košmrlj, *Org. Lett.*, 2020, **22**, 2157.
38. C. Erken, C. Hindemith, T. Weyhermüller, M. Hölscher, C. Werlé and W. Leitner, *ACS Omega*, 2020, **5**, 8912.
39. A. R. Shaffer and J. A. R. Schmidt, *Organometallics*, 2008, **27**, 1259.
40. K.-H. Yu, S.-L. Huang, Y.-H. Liu, Y. Wang, S.-T. Liu, Y.-C. Cheng, Y.-F. Lin and J.-T. Chen, *Molecules*, 2017, **22**, 1095.
41. Z. Zulu, G. S. Nyamato, T. A. Tshabalala and S. O. Ojwach, *Inorg. Chim. Acta*, 2020, **501**, 119270.

Received: 19th September 2022; Com. 22/7002